Review Article | Genitourinary Imaging

https://doi.org/10.3348/kjr.2018.19.2.193
pISSN 1229-6929 · eISSN 2005-8330
Korean J Radiol 2018;19(2):193-200

Korean Journal of Radiology
KJR

Prostate Imaging-Reporting and Data System Version 2: Beyond Prostate Cancer Detection

Sung Yoon Park, MD[1], Nam Hoon Cho, MD[2], Dae Chul Jung, MD[1], Young Taik Oh, MD[1]

Departments of [1]Radiology and [2]Pathology, Yonsei University College of Medicine, Seoul 03722, Korea

The main purpose of Prostate Imaging-Reporting and Data System Version 2 (PI-RADSv2) is to effectively detect clinically significant prostate cancers (csPCa) using multiparametric magnetic resonance imaging. Since the first introduction of PI-RADSv2, researchers have validated its diagnostic performance in identifying csPCa, and these promising data have influenced biopsy and treatment schemes. However, in this article, we focused on the potential of PI-RADSv2 in relation to various aspects of PCa such as Gleason score, tumor volume, extraprostatic extension, lymph node metastasis, and postoperative biochemical recurrence, beyond prostate cancer detection.

Keywords: *PI-RADS; Prostate cancer; Magnetic resonance imaging; Recurrence; Prognosis*

INTRODUCTION

Prostate Imaging-Reporting and Data System Version 2 (PI-RADSv2) is a language of prostate magnetic resonance imaging (MRI) for communicating the probability of clinically significant prostate cancer (csPCa). PI-RADSv2 scoring uses a 5-point Likert scale to assess csPCa, and study data have suggested that a score of 4 or greater indicates a high probability of csPCa (1, 2). The pooled sensitivity and specificity were 85–89% and 71–73%, respectively (2, 3).

In terms of estimating the likelihood of PCa, PI-RADSv2 scores are somewhat similar to prostate-specific antigen (PSA). The probability of PCa increases as the serum PSA level increases (e.g., < 4; 4–10; and ≥ 10) (4). Likewise, in recent studies, the detection rates of PCa increased sequentially according to PI-RADSv2 scores (5, 6). This situation indicates that PI-RADSv2 may provide guidelines with respect to further investigations such as biopsy, like PSA.

Prostatic lesions showing higher PI-RADSv2 scores are more likely to be proven as csPCa by targeted biopsy (7). Meanwhile, for the lesions with scores less than 3, an additional targeted biopsy may not be necessary because of low cancer detection rate (8). Also, the application of PI-RADSv2 may reduce the total number of biopsy cores. A previous study demonstrated comparable diagnostic performance between two-core targeted biopsy using PI-RADSv1 from prebiopsy MRI and 12-core systematic biopsy in detecting csPCa (9). For biopsy-proven low-grade PCa, PI-RADSv2 from postbiopsy MRI may aid in reducing the risk of underestimation by predicting the risk of Gleason score (GS) upgrading (10). This would aid in the decision regarding optimal management.

In PI-RADSv2, the lesions with higher scores, suggestive of csPCa, are likely to be apparently visible and/or large on multiparametric MRI (mpMRI) or surgical specimen. These radiologic and pathologic characteristics are inevitably associated with aggressiveness or prognosis of PCa (11, 12). Here, we will discuss the potential roles of PI-RADSv2

Received July 26, 2017; accepted after revision October 2, 2017.
Corresponding author: Young Taik Oh, MD, Department of Radiology, Yonsei University College of Medicine, 50 Yonsei-ro, Seodaemun-gu, Seoul 03722, Korea.
• Tel: (822) 2228-7400 • Fax: (822) 393-3035
• E-mail: oytaik@yuhs.ac

in assessing various aspects of PCa beyond its primary role in csPCa detection.

PI-RADSv2 Scoring and MRI Protocols

For PI-RADSv2 scoring, mpMRI consists of diffusion-weighted imaging (DWI) with/without dynamic contrast-enhanced (DCE) MRI for evaluating peripheral zone (PZ), and T2-weighted imaging (T2WI) with/without DWI for evaluating transition zone (TZ) (13). When the finding of the primary MR sequence is indeterminate for csPCa (e.g., a score of 3), findings of the secondary MR sequence (e.g., focal early enhancement in the DWI-suspected PZ lesion; focal areas of restricted diffusion, measuring 1.5 cm or greater, in the T2WI-suspected TZ lesion) can determine a final score of 3 or 4. The final PI-RADSv2 score using a 5-point scale is not for detecting every PCa, but for estimating the probability of csPCa.

It is recommended that some parameters of the essential MR sequences for scoring (e.g., T2WI, DWI, and DCE MRI) should be similar because they often have a complementary role in lesion characterization in the same prostatic region (14). At our institution, the field-of-view is uniformly 20 cm, and the slice thickness is 4 mm or less for the three MR sequences.

For acquiring an apparent diffusion coefficient (ADC) map, the monoexponential fit with the lowest b-value of 50–100 s/mm^2 and the highest b-value of 800–1000 s/mm^2 is appropriate. For analyzing high b-value DW images, PI-RADSv2 recommends image acquisition at a b-value of 1400–2000 s/mm^2 by means of either a direct or synthetic method because of better lesion conspicuity without significant loss of signal-to-noise ratio (15, 16).

In DCE MRI, a temporal resolution of 7 seconds or less is preferred to assess focal, early enhancement in the prostate gland (13). Semi-quantitative or quantitative analyses of DCE MRI using dedicated software are optional. T1-weighted imaging (T1WI) is also recommended to evaluate post-biopsy hemorrhage, delineate the gland, and detect lymph node (LN) or skeletal metastases although it is not integrated into the process of PI-RADSv2 scoring. The MRI protocols required for PI-RADSv2 interpretation have been well summarized in a previous review article (14).

Beyond Cancer Detection

Gleason Score

Analysis of DWI enables assessment of histologic tumor aggressiveness (17). Because the degree of restricted diffusion reflects the architectural distortion of the extracellular space and tumor cellularity (18), PCa with higher GS typically manifests as a focal hyperintense lesion on high b-value DWI with low ADC value. Hence, there is an inverse correlation between tumor ADC and GS. In visual analysis of DWI, lesion conspicuity is greatly affected by differences in restricted diffusion between cancerous and benign tissues (19). Thus, PCa with higher GS and diffusion restriction shows good lesion conspicuity on DWI.

In PI-RADSv2, DWI is a major MR sequence for PZ evaluation, and it also determines the likelihood of csPCa when the findings of T2WI are equivocal for TZ (e.g., a T2WI score of 3) (13). Therefore, PI-RADSv2 scores are closely associated with lesion conspicuity on DWI. Based on this background, a certain degree of relationship among the

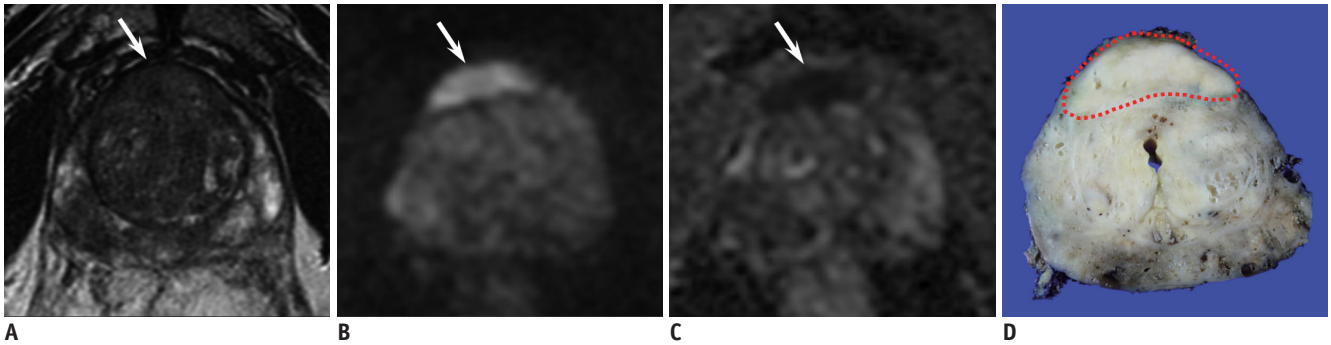

Fig. 1. 69-year-old man with serum PSA level of 18.6 ng/mL and biopsy-proven GS 6 PCa.
A. T2WI showed focal hypointense area in anterior TZ of prostate gland (arrow). PI-RADSv2 score on T2WI was 5. **B, C.** High b-value DWI and ADC map consistently showed focal area of diffusion restriction at corresponding site (arrow). Final PI-RADSv2 score on DWI was 5. Thus, final PI-RADSv2 score was 5 for TZ lesion. **D.** In surgical specimen, GS 7 PCa was confirmed (dotted area). This is case of GS upgrading, which was suspected by PI-RADSv2. ADC = apparent diffusion coefficient, DWI = diffusion-weighted imaging, GS = Gleason score, PCa = prostate cancer, PI-RADSv2 = Prostate Imaging-Reporting and Data System Version 2, PSA = prostate-specific antigen, TZ = transition zone, T2WI = T2-weighted imaging

Korean Journal of Radiology
KJR

degree of diffusion restriction, PI-RADSv2 scores, and GS is expected. In recent studies, PI-RADSv2 scores showed a positive correlation with GS (20). This helps PI-RADSv2 to verify the biopsy results (10, 21) (Fig. 1).

However, it is still uncertain which MR parameter is better correlated with GS. Basically, the interval of PI-RADSv2 scores is much greater than that of ADC values. Therefore, a particular score of PI-RADSv2 may comprise various ranges of GS (1) (Fig. 2). Conversely, there also may be a significant overlap of GS between neighboring PI-RADSv2 scores. For determining whether the PI-RADSv2 score is 4 or 5, the lesion size is an important factor (e.g., 1.5 cm). Thus, for GS 7 or greater PCa, the PI-RADSv2 score can be 4 when the tumor is small, while the score can be 5 when the tumor is large. Further studies are required to confirm which parameter better represents GS.

Tumor Volume

A tumor volume of 0.5 cm^3 is the most commonly applied threshold to determine csPCa (22). However, mpMRI is inadequate for detecting small PCa. Tumor volume less than 1.0 cm^3 is often associated with false negative diagnosis by means of mpMRI (23, 24). In addition, there are many benign mimickers in the prostate gland simulating PCa such as focal inflammation, stromal hyperplasia, central zone, anterior fibromuscular stroma, or surgical capsule (25). Thus, in case of a small PCa, there is a risk of false positive diagnosis by using mpMRI (e.g., a false diagnosis of the anterior fibromuscular stroma as a large anterior TZ PCa).

Vargas et al. (26) reported that more than 50% of PCa with GS 4 + 3 or greater were underestimated by PI-RADSv2 when the tumor volume is less than 0.5 cm^3. Seo et al. (10) reported that more than half of the underestimated cases (e.g., PI-RADSv2 score less than 4 for csPCa) had tumor volume less than 1.0 cm^3. Based on these data, there may be a discrepancy in the cutoff value of tumor volume between MR detectability and Epstein criteria (Fig. 3).

Multiparametric magnetic resonance imaging may also

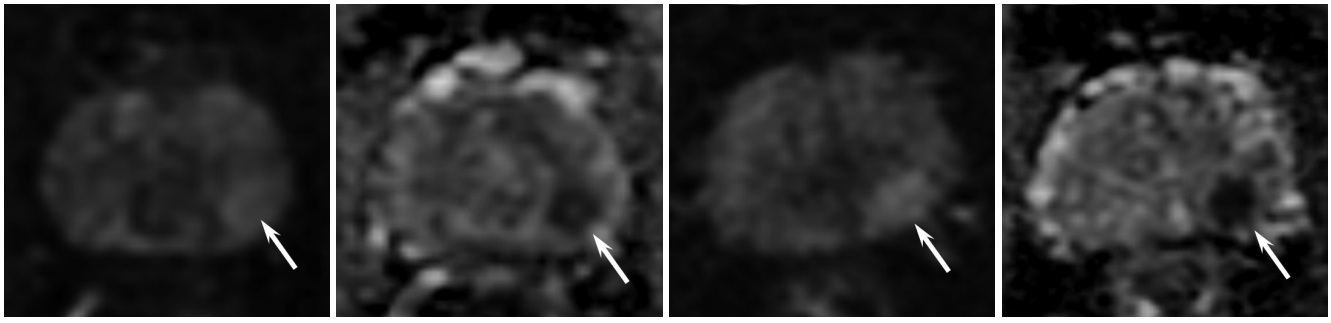

Fig. 2. DWI and ADC maps of two different patients.
A, B. 53-year-old man with serum PSA level of 7.6 ng/mL and PCa. High b-value DWI and ADC map showed focal area of diffusion restriction, measuring 0.9 cm, in left PZ of prostate gland (arrow). DWI and final PI-RADSv2 scores were 4 each. Mean tumor ADC was 0.91 x 10^{-3} mm^2/s. Surgery revealed GS 6 PCa. **C, D.** 65-year-old man with serum PSA level of 13.2 ng/mL and PCa. High b-value DWI and ADC map showed focal area of diffusion restriction, measuring 1.0 cm, in left PZ of prostate gland (arrow). DWI and final PI-RADSv2 scores were 4 each. Mean tumor ADC was 0.71 x 10^{-3} mm^2/s. Surgery revealed GS 7 PCa. These are cases of PCa with different GS, whose PI-RADSv2 scores were same, but tumor ADCs were different. PZ = peripheral zone

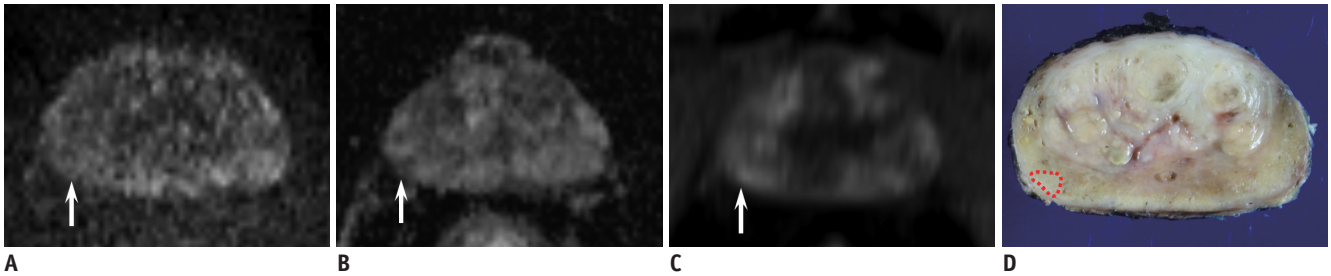

Fig. 3. 67-year-old man with serum PSA level of 22.4 ng/mL and PCa.
A, B. High b-value DWI and ADC map showed focal, indistinct area of mild diffusion restriction in right PZ of prostate gland (arrow). DWI score was 2. **C.** DCE MRI showed diffuse, gradual enhancement around corresponding site (arrow), which is suggestive of negative findings. Thus, final PI-RADSv2 score on DWI was 2 for PZ lesion. **D.** In surgical specimen, GS 6 PCa with tumor volume of 0.8 cm^3 was confirmed (dotted area). According to Epstein criteria, this is case of csPCa underestimated by PI-RADSv2. CsPCa = clinically significant prostate cancer, DCE = dynamic contrast-enhanced, MRI = magnetic resonance imaging

have a limitation in detecting sparse PCa. Sparse PCa consist of a mixture of scattered cancer cells and normal PZ tissues (27). Therefore, the volume of cancer cells in sparse PCa is inevitably smaller than that in dense PCs within the same region. Accordingly, it is expected that sparse PCa cannot be easily differentiated from adjacent normal prostatic tissues. Langer et al. (27) reported that ADC and T2 values of sparse PCas are similar to those of normal PZ tissues.

Based on these data, it should be determined whether the current Epstein criteria (1) GS > 3 + 3; 2) tumor volume ≥ 0.5 cm^3; or 3) presence of extraprostatic extension [EPE]), especially for the tumor volume, are indeed the appropriate goal of PI-RADSv2, or they need to be changed: for example, 1) GS 3 + 3 PCa with tumor volume ≥ 1.0 cm^3 or GS ≥ 3 + 4 PCa with any volume, or 2) only GS ≥ 3 + 4 PCa. Clinically, there is a debate regarding the tumor volume threshold for defining csPCa (28-30).

Extraprostatic Extension

Extraprostatic extension is a well-established adverse prognostic factor in PCa (31). Thus, radiologic investigation for EPE is important in terms of predicting the prognosis and surgical planning. The MR findings of organ-confined PCa may lead to a nerve-sparing approach in surgery (32). Conversely, a more wide excision may be required to secure the safety margins when EPE is highly suspected. In prostate MRI, T2WI is the mainstay for assessing EPE because of its high spatial resolution (13, 33).

The imaging criteria for EPE suggested in PI-RADSv2 are as follows (13): 1) asymmetry or invasion of the neurovascular bundles, 2) a bulging prostatic contour, 3) irregular or spiculated margin, 4) obliteration of the recto-prostatic angle, 5) a tumor-capsule interface of greater than 1 cm, or 6) breach of the capsule with evidence of direct tumor extension or bladder wall invasion. In PI-RADSv2, the findings of definite EPE on a major MR sequence (e.g., DWI for PZ and T2WI for TZ) lead to a final score of 5.

In a previous study conducted by Kayat Bittencourt et al. (34), the analysis of a major MR sequence alone allowed comparable performance with combined analysis of mpMRI for EPE. Another study demonstrated that a score of 5 showed higher rates of EPE than a score of 4 (48.7% vs. 11.5%; $p < 0.001$) (35). Krishna et al. (36) also found that the rate of EPE sequentially and significantly increased according to PI-RADSv2 scores. These data indicate that PI-RADSv2 has the potential to assess the risk of EPE.

However, there may be controversy regarding the imaging criteria for 'definite' EPE because the degree of suspicion may be relatively different for each MR criterion. For example, measurable extracapsular extension may be a stronger indicator than findings of capsular abutment or irregularity caused by cancer (37). Also, MR findings of subtle capsular or extracapsular changes could be inconsistently interpreted depending on the discretion of radiologists (Figs. 4, 5). Furthermore, integrating T2WI in the evaluation of EPE is somewhat discordant with the dictionary definition of 'definite EPE on DWI' when PZ is evaluated. More discussions regarding the definition of 'definite EPE' may be required as the current PI-RADSv2 only provides various imaging findings of EPE without any specific grading system for each finding unlike the initial version of PI-RADS.

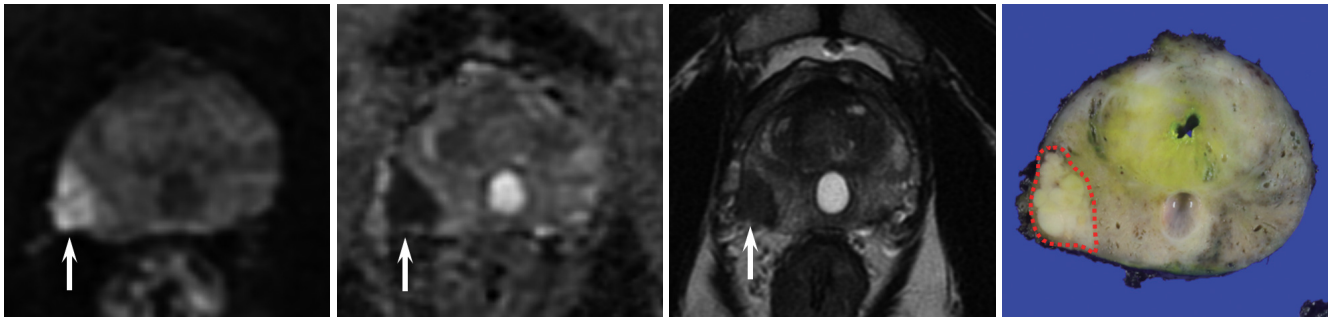

Fig. 4. 54-year-old man with serum PSA level of 6.2 ng/mL and PCa.
A, B. High b-value DWI and ADC map showed focal area of marked diffusion restriction, measuring 1.5 cm, in right PZ of prostate gland (arrow). Overt protrusion of lesion into right extraprostatic area was also seen. DWI score was consistently 5 as measured by two independent, experienced radiologists. **C.** T2WI also demonstrated focal hypointense lesion with high suspicion of right EPE (arrow). Thus, final PI-RADSv2 score on DWI was also consistently 5 for PZ lesion as measured by two independent, experienced radiologists. **D.** In surgical specimen, GS 8 PCa with right EPE was confirmed (dotted area). EPE = extraprostatic extension

Korean Journal of Radiology
KJR

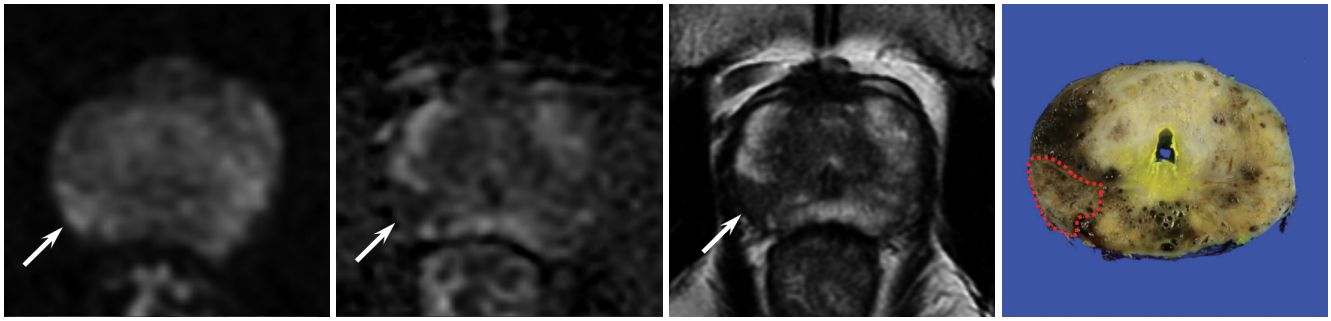

Fig. 5. 44-year-old man with serum PSA level of 22.0 ng/mL and PCa.
A, B. High b-value DWI and ADC map showed focal area of marked diffusion restriction, measuring 1.1 cm, in right PZ of prostate gland (arrow). Broad tumor-capsule contact was also seen. DWI score was 4 and 5 as measured by two independent, experienced radiologists, respectively, due to different interpretation regarding definite EPE. **C.** T2WI also demonstrated focal hypointense lesion with broad tumor-capsule contact (arrow). Thus, final PI-RADSv2 score on DWI was also 4 and 5 as measured by two independent, experienced radiologists, respectively. **D.** In surgical specimen, GS 7 PCa without EPE was confirmed (dotted area).

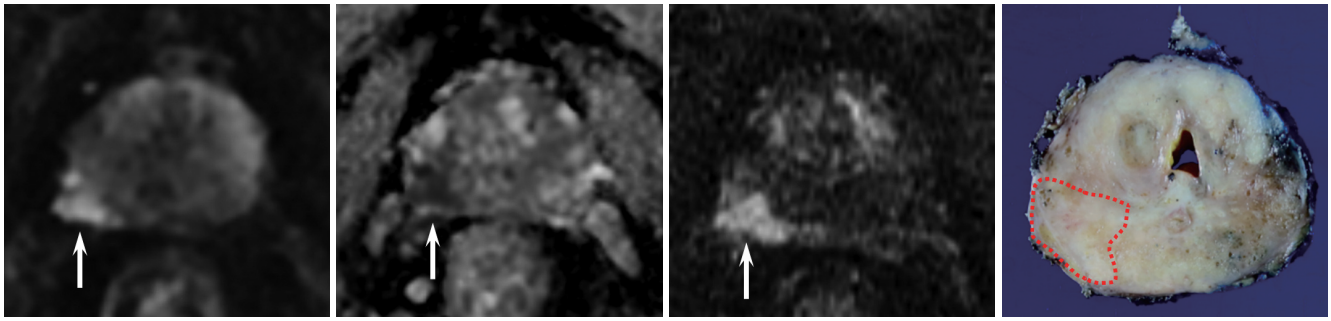

Fig. 6. 69-year-old man with serum PSA level of 19.7 ng/mL and PCa.
A, B. High b-value DWI and ADC map showed focal area of marked diffusion restriction, measuring 1.8 cm, in right PZ of prostate gland (arrow). Overt protrusion of lesion into right extraprostatic area was also seen. DWI score was 5. **C.** DCE MRI also showed positive findings (arrow). Thus, final PI-RADSv2 score was 5. **D.** In surgical specimen, GS 9 PCa with right EPE was confirmed (dotted area). In this patient, normal-sized (e.g., short-axis diameter < 0.8 cm) pelvic lymph node metastasis was proven surgically.

Lymph Node Metastasis

The status of pelvic LNs influences treatment planning. However, the currently available most optimal method for LN assessment is surgical LN dissection (32). Radiologically, pelvic LN metastases in PCa are often small (38). Thus, the use of the classical size criterion (e.g., 0.8–1.0 cm in short-axis diameter) alone is associated with the risk of underestimation in LN assessment (39, 40).

Previous studies have shown great promise in terms of advanced LN imaging: 1) MRI using ultra-small particles of iron oxide or 2) choline-based or prostate specific membrane antigen-based positron emission tomography scan (41-45). However, these techniques have not been utilized at every institution (46). Therefore, the selection of optimal candidates to maximize the effectiveness of advanced imaging or pelvic LN dissection (PLND) is important in daily practice, as it reduces the medical cost or morbidity.

In practice, various clinical nomograms aid in selecting the patients who need PLND. The parameters used in nomograms are usually PSA, clinical stage, and biopsy information including GS and tumor burden (47-49). Thus, the status of the primary lesion is closely related to the nodal status (11, 50). However, these parameters (e.g., stage, GS, or tumor burden) do not directly provide information regarding the anatomical status of PCa, thus miscalculation of the risk can occur (51).

As discussed earlier, PI-RADSv2 scores are associated with the status of GS, tumor volume, and EPE of PCa. Thus, there may be a certain degree of relationship between PI-RADSv2 scores and risk of pelvic LN metastasis. A recent study demonstrated that PSA, GS, and tumor stage were significantly different between patients with a score of 5 and the other patients (52). In the study, a cutoff score of 5 provided a positive predictive value of approximately

20%, while the negative predictive value was roughly 99% for normal-sized LN metastasis (Fig. 6). Therefore, the authors suggested that PI-RADSv2 may help predict a very low risk group for LN metastasis. Prospective validation is necessary for practical application.

Postoperative Biochemical Recurrence

Literatures have suggested that mpMRI may predict post-treatment prognosis following surgical (12) or non-surgical (53) treatment. Apparently visible lesions are more likely to be aggressive PCa with worse clinical outcomes, compared with PCa with poor lesion conspicuity. Zhang et al. (54) reported that PI-RADS version 1 was independently associated with time to biochemical recurrence (BCR), and adding the MR parameters to the clinical nomogram significantly increased the performance. Park et al. (20) reported that the 2-year BCR-free survival rates were significantly different among three PI-RADSv2 subgroups (approximately, 100% for patients with score 1–3; 90% for patients with score 4; and 70% for patients with score 5). This might be because various pathologic conditions of an index tumor or the risk of nodal invasion is reflected in PI-RADSv2. From this point of view, PI-RADSv2 may be one of the useful predictors for postoperative BCR. Long-term follow-up data and combined analysis of PI-RADSv2 scores with clinical parameters are currently necessary.

CONCLUSION

Prostate Imaging-Reporting and Data System Version 2 is an emerging tool for interpreting prostate MRI and it needs further validation regarding various aspects of PCa. Nevertheless, the data so far are promising. Based on the data discussed in this article, PI-RADSv2 seems to reflect tumor GS, tumor volume, EPE, nodal status, and postoperative BCR. Combined analysis of PI-RADSv2 scores with clinical parameters may maximize its effectiveness and may help in management planning. Therefore, as a non-invasive tool, PI-RADSv2 may play a role in evaluating various aspects of PCa as well as in detecting csPCa.

REFERENCES

1. Park SY, Jung DC, Oh YT, Cho NH, Choi YD, Rha KH, et al. Prostate cancer: PI-RADS version 2 helps preoperatively predict clinically significant cancers. *Radiology* 2016;280:108-116
2. Woo S, Suh CH, Kim SY, Cho JY, Kim SH. Diagnostic performance of prostate imaging reporting and data system version 2 for detection of prostate cancer: a systematic review and diagnostic meta-analysis. *Eur Urol* 2017;72:177-188
3. Zhang L, Tang M, Chen S, Lei X, Zhang X, Huan Y. A meta-analysis of use of prostate imaging reporting and data system version 2 (PI-RADS V2) with multiparametric MR imaging for the detection of prostate cancer. *Eur Radiol* 2017;27:5204-5214
4. van As NJ, Norman AR, Thomas K, Khoo VS, Thompson A, Huddart RA, et al. Predicting the probability of deferred radical treatment for localised prostate cancer managed by active surveillance. *Eur Urol* 2008;54:1297-1305
5. Mehralivand S, Bednarova S, Shih JH, Mertan FV, Gaur S, Merino MJ, et al. Prospective evaluation of PI-RADS™ version 2 using the international society of urological pathology prostate cancer grade group system. *J Urol* 2017;198:583-590
6. Martorana E, Pirola GM, Scialpi M, Micali S, Iseppi A, Bonetti LR, et al. Lesion volume predicts prostate cancer risk and aggressiveness: validation of its value alone and matched with prostate imaging reporting and data system score. *BJU Int* 2017;120:92-103
7. Tan N, Lin WC, Khoshnoodi P, Asvadi NH, Yoshida J, Margolis DJ, et al. In-Bore 3-T MR-guided transrectal targeted prostate biopsy: prostate imaging reporting and data system version 2-based diagnostic performance for detection of prostate cancer. *Radiology* 2017;283:130-139
8. Washino S, Okochi T, Saito K, Konishi T, Hirai M, Kobayashi Y, et al. Combination of prostate imaging reporting and data system (PI-RADS) score and prostate-specific antigen (PSA) density predicts biopsy outcome in prostate biopsy naive patients. *BJU Int* 2017;119:225-233
9. Baco E, Rud E, Eri LM, Moen G, Vlatkovic L, Svindland A, et al. A randomized controlled trial to assess and compare the outcomes of two-core prostate biopsy guided by fused magnetic resonance and transrectal ultrasound images and traditional 12-core systematic biopsy. *Eur Urol* 2016;69:149-156
10. Seo JW, Shin SJ, Taik Oh Y, Jung DC, Cho NH, Choi YD, et al. PI-RADS version 2: detection of clinically significant cancer in patients with biopsy gleason score 6 prostate cancer. *AJR Am J Roentgenol* 2017;209:W1-W9
11. Abdollah F, Suardi N, Gallina A, Bianchi M, Tutolo M, Passoni N, et al. Extended pelvic lymph node dissection in prostate cancer: a 20-year audit in a single center. *Ann Oncol* 2013;24:1459-1466
12. Park JJ, Kim CK, Park SY, Park BK, Lee HM, Cho SW. Prostate cancer: role of pretreatment multiparametric 3-T MRI in predicting biochemical recurrence after radical prostatectomy. *AJR Am J Roentgenol* 2014;202:W459-W465
13. Weinreb JC, Barentsz JO, Choyke PL, Cornud F, Haider MA, Macura KJ, et al. PI-RADS prostate imaging - reporting and data system: 2015, version 2. *Eur Urol* 2016;69:16-40
14. Fütterer JJ. Multiparametric MRI in the detection of clinically significant prostate cancer. *Korean J Radiol* 2017;18:597-606
15. Maas MC, Fütterer JJ, Scheenen TW. Quantitative evaluation

of computed high B value diffusion-weighted magnetic resonance imaging of the prostate. *Invest Radiol* 2013;48:779-786
16. Ueno Y, Takahashi S, Kitajima K, Kimura T, Aoki I, Kawakami F, et al. Computed diffusion-weighted imaging using 3-T magnetic resonance imaging for prostate cancer diagnosis. *Eur Radiol* 2013;23:3509-3516
17. Vargas HA, Akin O, Franiel T, Mazaheri Y, Zheng J, Moskowitz C, et al. Diffusion-weighted endorectal MR imaging at 3 T for prostate cancer: tumor detection and assessment of aggressiveness. *Radiology* 2011;259:775-784
18. Chatterjee A, Watson G, Myint E, Sved P, McEntee M, Bourne R. Changes in epithelium, stroma, and lumen space correlate more strongly with gleason pattern and are stronger predictors of prostate ADC changes than cellularity metrics. *Radiology* 2015;277:751-762
19. Park SY, Shin SJ, Jung DC, Cho NH, Choi YD, Rha KH, et al. PI-RADS version 2: quantitative analysis aids reliable interpretation of diffusion-weighted imaging for prostate cancer. *Eur Radiol* 2017;27:2776-2783
20. Park SY, Oh YT, Jung DC, Cho NH, Choi YD, Rha KH, et al. Prediction of biochemical recurrence after radical prostatectomy with PI-RADS version 2 in prostate cancers: initial results. *Eur Radiol* 2016;26:2502-2509
21. Woo S, Kim SY, Lee J, Kim SH, Cho JY. PI-RADS version 2 for prediction of pathological downgrading after radical prostatectomy: a preliminary study in patients with biopsy-proven Gleason Score 7 (3+4) prostate cancer. *Eur Radiol* 2016;26:3580-3587
22. Ploussard G, Epstein JI, Montironi R, Carroll PR, Wirth M, Grimm MO, et al. The contemporary concept of significant versus insignificant prostate cancer. *Eur Urol* 2011;60:291-303
23. Vargas HA, Akin O, Shukla-Dave A, Zhang J, Zakian KL, Zheng J, et al. Performance characteristics of MR imaging in the evaluation of clinically low-risk prostate cancer: a prospective study. *Radiology* 2012;265:478-487
24. Le JD, Tan N, Shkolyar E, Lu DY, Kwan L, Marks LS, et al. Multifocality and prostate cancer detection by multiparametric magnetic resonance imaging: correlation with whole-mount histopathology. *Eur Urol* 2015;67:569-576
25. Kitzing YX, Prando A, Varol C, Karczmar GS, Maclean F, Oto A. Benign conditions that mimic prostate carcinoma: MR imaging features with histopathologic correlation. *Radiographics* 2016;36:162-175
26. Vargas HA, Hötker AM, Goldman DA, Moskowitz CS, Gondo T, Matsumoto K, et al. Updated prostate imaging reporting and data system (PIRADS v2) recommendations for the detection of clinically significant prostate cancer using multiparametric MRI: critical evaluation using whole-mount pathology as standard of reference. *Eur Radiol* 2016;26:1606-1612
27. Langer DL, van der Kwast TH, Evans AJ, Sun L, Yaffe MJ, Trachtenberg J, et al. Intermixed normal tissue within prostate cancer: effect on MR imaging measurements of apparent diffusion coefficient and T2--sparse versus dense cancers. *Radiology* 2008;249:900-908
28. Wolters T, Roobol MJ, van Leeuwen PJ, van den Bergh RC, Hoedemaeker RF, van Leenders GJ, et al. A critical analysis of the tumor volume threshold for clinically insignificant prostate cancer using a data set of a randomized screening trial. *J Urol* 2011;185:121-125
29. Ting F, van Leeuwen PJ, Delprado W, Haynes AM, Brenner P, Stricker PD. Tumor volume in insignificant prostate cancer: Increasing the threshold is a safe approach to reduce over-treatment. *Prostate* 2015;75:1768-1773
30. Kryvenko ON, Epstein JI. Definition of insignificant tumor volume of gleason score 3 + 3 = 6 (grade group 1) prostate cancer at radical prostatectomy-is it time to increase the threshold? *J Urol* 2016;196:1664-1669
31. Kattan MW, Wheeler TM, Scardino PT. Postoperative nomogram for disease recurrence after radical prostatectomy for prostate cancer. *J Clin Oncol* 1999;17:1499-1507
32. Mottet N, Bellmunt J, Bolla M, Briers E, Cumberbatch MG, De Santis M, et al. EAU-ESTRO-SIOG guidelines on prostate cancer. Part 1: screening, diagnosis, and local treatment with curative intent. *Eur Urol* 2017;71:618-629
33. Gupta RT, Spilseth B, Patel N, Brown AF, Yu J. Multiparametric prostate MRI: focus on T2-weighted imaging and role in staging of prostate cancer. *Abdom Radiol (NY)* 2016;41:831-843
34. Kayat Bittencourt L, Litjens G, Hulsbergen-van de Kaa CA, Turkbey B, Gasparetto EL, Barentsz JO. Prostate cancer: the European society of urogenital radiology prostate imaging reporting and data system criteria for predicting extraprostatic extension by using 3-T multiparametric MR imaging. *Radiology* 2015;276:479-489
35. Lim CS, McInnes MDF, Lim RS, Breau RH, Flood TA, Krishna S, et al. Prognostic value of Prostate Imaging and Data Reporting System (PI-RADS) v. 2 assessment categories 4 and 5 compared to histopathological outcomes after radical prostatectomy. *J Magn Reson Imaging* 2017;46:257-266
36. Krishna S, Lim CS, McInnes MDF, Flood TA, Shabana WM, Lim RS, et al. Evaluation of MRI for diagnosis of extraprostatic extension in prostate cancer. *J Magn Reson Imaging* 2018;47:176-185
37. Matsuoka Y, Ishioka J, Tanaka H, Kimura T, Yoshida S, Saito K, et al. Impact of the Prostate Imaging Reporting and Data System, Version 2, on MRI diagnosis for extracapsular extension of prostate cancer. *AJR Am J Roentgenol* 2017;209:W76-W84
38. McMahon CJ, Rofsky NM, Pedrosa I. Lymphatic metastases from pelvic tumors: anatomic classification, characterization, and staging. *Radiology* 2010;254:31-46
39. Hövels AM, Heesakkers RA, Adang EM, Jager GJ, Strum S, Hoogeveen YL, et al. The diagnostic accuracy of CT and MRI in the staging of pelvic lymph nodes in patients with prostate cancer: a meta-analysis. *Clin Radiol* 2008;63:387-395
40. Briganti A, Abdollah F, Nini A, Suardi N, Gallina A, Capitanio U, et al. Performance characteristics of computed tomography in detecting lymph node metastases in contemporary patients

with prostate cancer treated with extended pelvic lymph node dissection. *Eur Urol* 2012;61:1132-1138
41. Harisinghani MG, Barentsz J, Hahn PF, Deserno WM, Tabatabaei S, van de Kaa CH, et al. Noninvasive detection of clinically occult lymph-node metastases in prostate cancer. *N Engl J Med* 2003;348:2491-2499
42. Thoeny HC, Triantafyllou M, Birkhaeuser FD, Froehlich JM, Tshering DW, Binser T, et al. Combined ultrasmall superparamagnetic particles of iron oxide-enhanced and diffusion-weighted magnetic resonance imaging reliably detect pelvic lymph node metastases in normal-sized nodes of bladder and prostate cancer patients. *Eur Urol* 2009;55:761-769
43. Birkhäuser FD, Studer UE, Froehlich JM, Triantafyllou M, Bains LJ, Petralia G, et al. Combined ultrasmall superparamagnetic particles of iron oxide-enhanced and diffusion-weighted magnetic resonance imaging facilitates detection of metastases in normal-sized pelvic lymph nodes of patients with bladder and prostate cancer. *Eur Urol* 2013;64:953-960
44. Vag T, Heck MM, Beer AJ, Souvatzoglou M, Weirich G, Holzapfel K, et al. Preoperative lymph node staging in patients with primary prostate cancer: comparison and correlation of quantitative imaging parameters in diffusion-weighted imaging and 11C-choline PET/CT. *Eur Radiol* 2014;24:1821-1826
45. Herlemann A, Wenter V, Kretschmer A, Thierfelder KM, Bartenstein P, Faber C, et al. 68Ga-PSMA positron emission tomography/computed tomography provides accurate staging of lymph node regions prior to lymph node dissection in patients with prostate cancer. *Eur Urol* 2016;70:553-557
46. Hövels AM, Heesakkers RA, Adang EM, Jager GJ, Barentsz JO. Cost-analysis of staging methods for lymph nodes in patients with prostate cancer: MRI with a lymph node-specific contrast agent compared to pelvic lymph node dissection or CT. *Eur Radiol* 2004;14:1707-1712
47. Briganti A, Larcher A, Abdollah F, Capitanio U, Gallina A, Suardi N, et al. Updated nomogram predicting lymph node invasion in patients with prostate cancer undergoing extended pelvic lymph node dissection: the essential importance of percentage of positive cores. *Eur Urol* 2012;61:480-487
48. Cagiannos I, Karakiewicz P, Eastham JA, Ohori M, Rabbani F, Gerigk C, et al. A preoperative nomogram identifying decreased risk of positive pelvic lymph nodes in patients with prostate cancer. *J Urol* 2003;170:1798-1803
49. Kim KH, Lim SK, Kim HY, Han WK, Choi YD, Chung BH, et al. Yonsei nomogram to predict lymph node invasion in Asian men with prostate cancer during robotic era. *BJU Int* 2014;113:598-604
50. Paño B, Sebastià C, Buñesch L, Mestres J, Salvador R, Macías NG, et al. Pathways of lymphatic spread in male urogenital pelvic malignancies. *Radiographics* 2011;31:135-160
51. Zhang J, Hricak H, Shukla-Dave A, Akin O, Ishill NM, Carlino LJ, et al. Clinical stage T1c prostate cancer: evaluation with endorectal MR imaging and MR spectroscopic imaging. *Radiology* 2009;253:425-434
52. Park SY, Shin SJ, Jung DC, Cho NH, Choi YD, Rha KH, et al. PI-RADS version 2: preoperative role in the detection of normal-sized pelvic lymph node metastasis in prostate cancer. *Eur J Radiol* 2017;91:22-28
53. Fuchsjäger MH, Pucar D, Zelefsky MJ, Zhang Z, Mo Q, Ben-Porat LS, et al. Predicting post-external beam radiation therapy PSA relapse of prostate cancer using pretreatment MRI. *Int J Radiat Oncol Biol Phys* 2010;78:743-750
54. Zhang YD, Wu CJ, Bao ML, Li H, Wang XN, Liu XS, et al. MR-based prognostic nomogram for prostate cancer after radical prostatectomy. *J Magn Reson Imaging* 2017;45:586-596